

Squeezed light from a silicon micromechanical resonator

Amir H. Safavi-Naeini^{1,2*}, Simon Gröblacher^{1,2*}, Jeff T. Hill^{1,2*}, Jasper Chan¹, Markus Aspelmeyer³ & Oskar Painter^{1,2,4}

Monitoring a mechanical object's motion, even with the gentle touch of light, fundamentally alters its dynamics. The experimental manifestation of this basic principle of quantum mechanics, its link to the quantum nature of light and the extension of quantum measurement to the macroscopic realm have all received extensive attention over the past half-century^{1,2}. The use of squeezed light, with quantum fluctuations below that of the vacuum field, was proposed nearly three decades ago³ as a means of reducing the optical read-out noise in precision force measurements. Conversely, it has also been proposed that a continuous measurement of a mirror's position with light may itself give rise to squeezed light^{4,5}. Such squeezed-light generation has recently been demonstrated in a system of ultracold gas-phase atoms⁶ whose centre-of-mass motion is analogous to the motion of a mirror. Here we describe the continuous position measurement of a solid-state, optomechanical system fabricated from a silicon microchip and comprising a micromechanical resonator coupled to a nanophotonic cavity. Laser light sent into the cavity is used to measure the fluctuations in the position of the mechanical resonator at a measurement rate comparable to its resonance frequency and greater than its thermal decoherence rate. Despite the mechanical resonator's highly excited thermal state (10⁴ phonons), we observe, through homodyne detection, squeezing of the reflected light's fluctuation spectrum at a level 4.5 ± 0.2 per cent below that of vacuum noise over a bandwidth of a few megahertz around the mechanical resonance frequency of 28 megahertz. With further device improvements, on-chip squeezing at significant levels should be possible, making such integrated microscale devices well suited for precision metrology applications.

The generation of states of light with fluctuations below that of vacuum has been of great theoretical interest since the 1970s^{3,7-9}. Early experimental work demonstrated squeezing of a few per cent below the vacuum noise level in a large variety of different nonlinear systems, such as neutral atoms in a cavity¹⁰, optical fibres¹¹ and crystals with bulk optical nonlinearities^{12,13}. Modern experiments demonstrate squeezing of almost 13 dB (ref. 14). Initial research was mainly pursued as a strategy to mitigate the effects of shot-noise, the manifestation of vacuum noise in the intensity detection of light, given the possibility of improved optical communication⁷ and better sensitivity in gravitational-wave detectors^{3,8}. In recent years, in addition to being used in gravitational-wave detectors¹⁵, squeezed light has enhanced metrology in more applied settings^{16,17}.

The vacuum fluctuations arising from the quantum nature of light determine our ability to resolve mechanical motion optically, and set limits on the perturbation caused by the act of measurement of system well suited to studying quantum measurement experimentally is that of cavity optomechanics, in which an optical cavity's resonance frequency is designed to be sensitive to the position of a mechanical system. By monitoring the phase and intensity of the reflected light from such a cavity, a continuous measurement of mechanical displacement can be made. Systems operating on this simple principle have been realized in a variety of experimental settings, such as in large-scale laser gravitational-wave interferometers of microwave circuits with

electromechanical elements²⁰, solid-state mechanical elements^{21–23} and ultracold gas-phase atoms^{6,24} integrated with or comprising Fabry–Pérot cavities, and on-chip nanophotonic cavities sensitive to mechanical deformations^{25,26}.

The canonical cavity-optomechanical system consists of an optical cavity resonance that is dispersively coupled to the position of a mechanical resonance. The Hamiltonian describing the interaction between light and mechanics is $H_{\text{int}} = \hbar g_0 \hat{a}^{\dagger} \hat{a} \hat{x} / x_{\text{zpf}}$, where $\hat{x} = x_{\text{zpf}} (\hat{b}^{\dagger} + \hat{b})$ is the mechanical position, $x_{\rm zpf} = \sqrt{\hbar/2m_{\rm eff}\omega_{\rm m}}$ is the zero-point fluctuation amplitude, $\omega_{\rm m}$ is the mechanical resonance frequency, $m_{\rm eff}$ is the effective motional mass of the resonator, g_0 is the frequency shift of the optical resonance for a mechanical amplitude of x_{zpf} , \hbar is Planck's constant divided by 2π , \hat{a} and \hat{a}^{\dagger} are respectively the annihilation and creation operators for optical excitations, and \hat{b} and \hat{b}^{\dagger} are the analogous operators for mechanical excitations. The optical cavity decay rate, κ , is the loss rate of photons from the cavity and the rate at which optical vacuum fluctuations are coupled into the optical resonance²⁷. Similarly, the mechanical damping rate, γ_i , is the rate at which thermal bath fluctuations couple to the mechanical system. In all experimental realizations of solid-state optomechanics so far, including that presented here, the optomechanical coupling rate, go, has been much smaller than κ . As such, without a strong coherent drive, the interaction of the vacuum fluctuations with the mechanics is negligible.

Under the effect of a coherent laser drive, the cavity is populated with a mean intracavity photon number $\langle n_c \rangle$, and we consider the optical fluctuations about the classical steady state, $\hat{a} \rightarrow \sqrt{\langle n_c \rangle} + \hat{a}$. This modifies the optomechanical interaction, resulting in a linear coupling between the fluctuations of the intracavity optical field, $\hat{X}_0 = \hat{a} + \hat{a}^{\dagger}$, and the position fluctuations of the mechanical system, \hat{x} : $H_{\rm int} = \hbar G \hat{X}_0 \hat{x} / x_{\rm zpf}$. The parametric linear coupling occurs at an effective interaction rate of $G \equiv \sqrt{\langle n_c \rangle} g_0$, and the mechanical motion is coupled to the intracavity optical field at a rate of $\Gamma_{\rm meas} \equiv 4 G^2 / \kappa$. Through this interaction, the intensity fluctuations of the vacuum field, $\hat{X}_{\theta=0}^{\rm (in)}(t)$, entering the cavity impart a force on the mechanical system:

$$\hat{F}_{BA}(t) = \frac{\hbar\sqrt{\Gamma_{\text{meas}}}}{x_{\text{rnf}}} \hat{X}_{\theta=0}^{(\text{in})}(t)$$
 (1)

This radiation-pressure shot-noise (RPSN) force has previously been measured in an ultracold atomic gas²⁴ and, more recently, on a macroscopic silicon nitride nanomembrane²⁸. The mechanical motion is in turn recorded in the phase of the light leaving the cavity:

$$\hat{X}_{\theta}^{(\text{out})}(t) = -\hat{X}_{\theta}^{(\text{in})}(t) - 2\frac{\sqrt{\Gamma_{\text{meas}}}}{x_{\text{zpf}}}\hat{x}(t)\sin(\theta)$$
 (2)

Here $\hat{X}^{(j)}_{\theta} = \hat{a}_j \mathrm{e}^{-i\theta} + \hat{a}_j^{\dagger} \mathrm{e}^{i\theta}$, \hat{a}_{in} and \hat{a}_{out} are respectively the operators of the input and reflected optical fields from the cavity, and θ is the quadrature angle with $\theta=0$ and $\theta=\pi/2$ corresponding respectively to the intensity and phase quadratures. In such a measurement, the optical cavity has the role of the position detector, measuring the observable \hat{x} at a rate Γ_{meas} , and the RPSN imposes a measurement back-action force on the mechanical system². In addition to this back-action noise, thermal

¹Kavli Nanoscience Institute and Thomas J. Watson, Sr, Laboratory of Applied Physics, California Institute of Technology, Pasadena, California 91125, USA. ²Institute for Quantum Information and Matter, California Institute of Technology, Pasadena, California 91125, USA. ³Vienna Center for Quantum Science and Technology, Faculty of Physics, University of Vienna, A-1090 Wien, Austria. ⁴Max Planck Institute for the Science of Light, Günther-Scharowsky-Straße 1/Bldg 24, D-91058 Erlangen, Germany.

^{*}These authors contributed equally to this work.

fluctuations from the bath also drive the mechanical motion, with their magnitudes becoming comparable as $\Gamma_{\rm meas}$ approaches the thermalization rate, $\Gamma_{\rm thermal}(\omega) \equiv \gamma_{\rm i} \bar{n}(\omega)$, where $\bar{n}(\omega)$ is the thermal bath occupancy.

Formally, the output noise power spectral density (PSD) of the homodyne detector photocurrent, I, normalized to the shot-noise level is found by taking the Fourier transform of the autocorrelation of equation (2):

$$\bar{S}_{II}^{\text{out}}(\omega) = 1 + \frac{4\Gamma_{\text{meas}}}{x_{\text{rat}}^2} \left[\bar{S}_{xx} \sin^2(\theta) + \frac{\hbar}{2} \text{Re}\{\chi_{\text{m}}\} \sin(2\theta) \right]$$
(3)

where $\bar{S}_{xx}(\omega)$ is the noise PSD of the mechanical position fluctuations of the resonator and $\chi_{\rm m}(\omega) = (m_{\rm eff}(\omega_{\rm m}^2 - \omega^2 - i\gamma_i\omega_{\rm m}))^{-1}$ is the mechanical susceptibility characterizing the response of the mechanical system to an applied force. The PSD $\bar{S}_{xx}(\omega)$ contains noise stemming from coupling to the thermal bath, quantum back-action noise from the light field and any other technical laser noise driving the mechanics (Supplementary Information). The three terms in $\bar{S}_{II}^{\rm out}(\omega)$ in equation (3), from left to right, are due to shot-noise, mechanical position fluctuations and the cross-correlation between the back-action noise force and mechanical position fluctuations. Only the third term can have a negative noise PSD and give rise to squeezing.

The primary hurdle to observing such squeezing, as in many quantum measurements, is strongly coupling to a preferred detection channel while simultaneously minimizing unwanted environmental perturbations. Most relevant to the work presented here are frequencies detuned from resonance, $\omega_{\rm m}\!>\!|\delta\equiv\omega_{\rm m}-\omega|\!\gg\!\gamma_{\rm i}$, for which the approximate output noise PSD is

$$\bar{S}_{II}^{\rm out}(\omega\!>\!0)\!\approx\!1+\frac{2\varGamma_{\rm meas}}{\delta}\left[\frac{\omega_{\rm m}}{\delta}\frac{\bar{n}(\omega)}{Q_{\rm m}}(1-\cos{(2\theta)})+\sin{(2\theta)}\right]$$

where we have assumed that the mechanical position fluctuations are predominantly due to thermal bath coupling (at high optical power, back-action heating and laser noise also contribute to the mode occupancy). In this case, fluctuations from the thermal bath limit appreciable squeezing of the optical probe field to a regime in which $\bar{n}(\omega)/Q_{\rm m} \lesssim 1$. This requirement is equivalent to having $Q_{\rm m}\omega_{\rm m}\gtrsim k_{\rm B}T_{\rm b}/\hbar$, where $k_{\rm B}$ is Boltzmann's constant and T_b is the bath temperature. Appreciable squeezing also requires a detuning $|\delta|\gtrsim (\bar{n}/Q_{\rm m})\omega_{\rm m}$ and a corresponding measurement rate larger than this detuning. Therefore, in the presence of thermal bath noise, squeezing over a significant spectral bandwidth requires not only a large cooperativity ($C \equiv \Gamma_{\text{meas}}/\gamma_i$) between the optical and mechanical components, as realized in recent cooling experiments^{20,26,29}, but the more stringent requirement that the effective measurement back-action force be comparable to all forces acting on the mechanical resonator, including the elastic restoring force of the mechanical structure.

To meet the requirements of strong measurement and efficient detection, we designed a 'zipper-style' optomechanical cavity' with a novel integrated waveguide coupler fabricated from the 220-nm-thick silicon device layer of a silicon-on-insulator microchip (Fig. 1). The in-plane differential motion of the two beams at a fundamental frequency of $\omega_{\rm m}/2\pi=28$ MHz strongly modulates the co-localized fundamental optical resonance of the cavity with a theoretical vacuum coupling rate of $g_0/2\pi=1$ MHz. As shown in Fig. 1b, we use a silicon waveguide with a high-reflectivity photonic crystal end-mirror to excite and collect light efficiently from the optical cavity. Light from the silicon waveguide is coupled to a single-mode optical fibre using an optical fibre taper and a combination of adiabatic mode coupling and transformation.

The experimental set-up used to characterize the zipper cavity system and measure the optomechanical squeezing of light is shown in Fig. 2a. The silicon sample is placed in a continuous-flow 4 He cryostat with a cold-finger temperature of 10 K. A narrowband laser beam is used to probe the optomechanical system and measure the mechanical

motion of the zipper cavity. A wavelength scan of the reflected signal from the cavity is plotted in Fig. 2b, showing an optical resonance with a linewidth $\kappa/2\pi=3.42\,\mathrm{GHz}$ at a wavelength of $\lambda_c=1,540\,\mathrm{nm}$. Inefficiencies in the collection and detection of light result in additional uncorrelated shot-noise in the measured signal and can reduce the squeezing to undetectable levels. For the device studied here, the cavity coupling efficiency, corresponding to the percentage of photons sent into the cavity which are reflected, is determined to be $\eta_\kappa=0.54$. The fibre-to-chip coupling efficiency is measured at $\eta_{\mathrm{CP}}=0.90$. A homodyne detection scheme allows for high-efficiency detection of arbitrary quadratures of the optical signal field. Characterization and optimization of the efficiency of the entire optical signal path and homodyne detection system yielded an overall set-up efficiency of $\eta_{\mathrm{set-up}}=0.48$, corresponding to a total signal detection efficiency of $\eta_{\mathrm{tot}}=\eta_{\mathrm{set-up}}\eta_\kappa=0.26$.

Figure 2c shows the noise spectrum of the thermal motion of the mechanical resonator obtained by setting the laser frequency near the cavity resonance and tuning the relative local-oscillator phase of the homodyne detector, θ_{lock} , to measure the quadrature of the reflected signal in which mechanical motion is imprinted. The mechanical spectrum shows the in-plane differential mode of interest at $\omega_{\rm m}$ $2\pi = 28$ MHz, as well as several other more weakly coupled mechanical resonances of the nanobeams and coupling waveguide. A highresolution, narrowband spectrum of the in-plane differential mode is inset in Fig. 2c, and shows a linewidth of $\gamma_i/2\pi = 172$ Hz, corresponding to a mechanical Q-factor of $Q_m = 1.66 \times 10^5$. The vacuum coupling rate of the in-plane differential mode, measured from the detuning dependence of the optical spring shift and damping, is determined to be $g_0/2\pi = 750 \,\text{kHz}$, in good agreement with theory. From the calibration of the noise power under the Lorentzian distribution in Fig. 2c, the in-plane differential mode is found to thermalize at low optical probe power to a temperature of $T_b \approx 16$ K, corresponding to a thermal phonon occupancy of $\bar{n}(\omega_{\rm m}) \approx 1.2 \times 10^4$. This yields a ratio

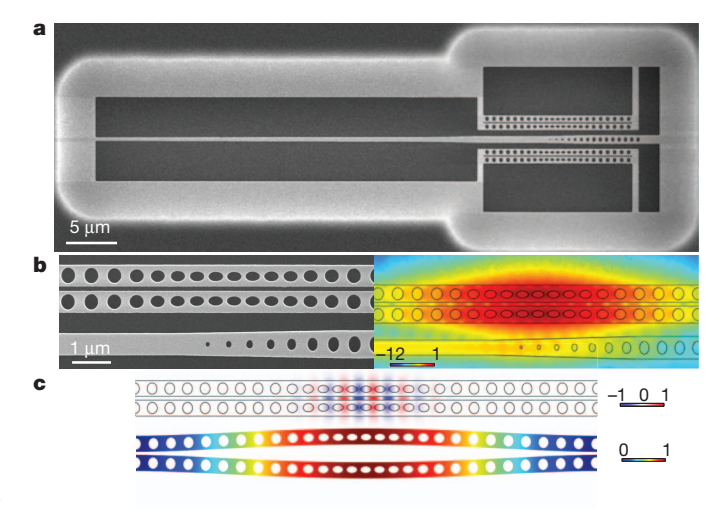


Figure 1 Optomechanical device. a, Scanning electron microscope image of a waveguide-coupled zipper optomechanical cavity. The waveguide width is adiabatically tapered along its length and terminates with a photonic crystal mirror next to the cavity. The tapering of the waveguide allows for efficient input-output coupling and the photonic crystal termination makes the coupling to the cavity single sided. Two zipper cavities are coupled above and below the waveguide, each with a slightly different optical resonance frequency, allowing them to be separately addressed. b, Left: close-up of the coupling region between one of the cavities and the waveguide. Right: finite-element method (FEM) simulation of the cavity field leaking into the waveguide (log scale). Note that the field does not leak into the mirror region of the waveguide. c, Top: FEM simulation showing the in-plane electrical field of the fundamental optical cavity mode. Bottom: FEM simulation of the displacement of the fundamental in-plane differential mode of the structure with frequency $\omega_{\mathrm{m}}/$ $2\pi = 28$ MHz. The mechanical motion, modifying the gap between the beams, shifts the optical cavity frequency, leading to optomechanical coupling.

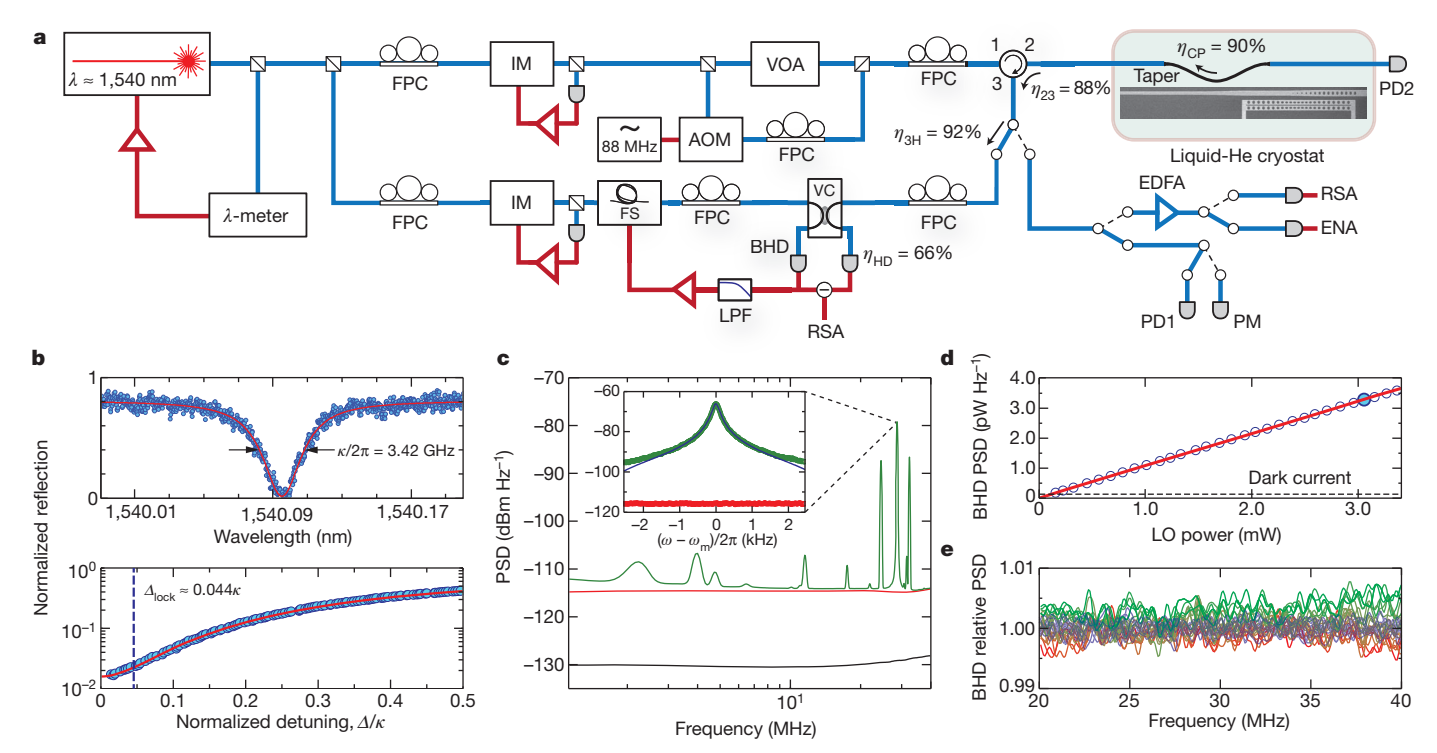


Figure 2 | Experimental set-up and device characterization. a, The optical signal is derived from an external-cavity diode laser and is sent into a tapered optical fibre inside a liquid-helium cryostat where the silicon sample is cooled to $T\approx 16$ K. The fibre taper is used to couple light evanescently into the silicon optomechanical device. The optical reflection from the device is collected by the same fibre taper and sent to a balanced homodyne detector (BHD) for characterization. For further details of the experimental set-up, see Methods Summary. The efficiencies of the circulator, switch and BHD are respectively denoted η_{23} , η_{3H} and η_{HD} . AOM, acousto-optic modulator; EDFA, erbium-doped fibre amplifier; ENA, electronic network analyser; FPC, fibre polarization controller; FS, fibre stretcher; IM, intensity modulator; λ -meter, wavemeter; LPF, low-pass filter; PD, photodetector; PM, power meter; RSA, real-time spectrum analyser; VC, variable coupler; VOA, variable optical attenuator. b, Top: reflected signal from the optical cavity at low optical power ($\langle n_c \rangle \approx 10$; linewidth, $\kappa/2\pi = 3.42$ GHz). Bottom: high-power ($\langle n_c \rangle = 790$)

 $\bar{\it n}(\omega_m)/Q_m{\approx}0.072,$ which is well within the regime where squeezing is possible.

To study accurately the noise properties of the reflected optical signal from the cavity, we make a series of measurements to characterize our laser and detection set-up. Figure 2d shows the measured noise PSD of the balanced homodyne detector for $\omega \approx \omega_{\rm m}$ as a function of local-oscillator power, indicating a linear dependence on power and negligible ($\ll 0.1\%$) added noise above shot-noise. In the measured squeezing data discussed below, a local-oscillator power of 3 mW is used. Calibration of the laser intensity and frequency noise over the frequency range of interest ($\omega/2\pi = 1-40 \,\mathrm{MHz}$) is described in Supplementary Information. The laser intensity noise is measured to be dominated by shot-noise over this frequency range, and the laser frequency noise is measured to be roughly flat in frequency at a level of $S_{\omega\omega} \approx 5 \times 10^3 \,\text{rad}^2 \,\text{Hz}$, which contributes insignificantly to the detected noise floor. Figure 2e shows the measured homodyne detector noise level normalized to vacuum noise for reflected laser light far-detuned from the optical cavity resonance. The small ($\sim \pm 0.15\%$) deviation in the measured noise level bounds the systematic uncertainty in the detector gain versus quadrature bias point as well as the contribution to the measured noise from optical elements other than the silicon cavity.

Measurements of the noise in the reflected optical signal from the cavity as a function of quadrature angle, frequency and signal power are shown in Figs 3 and 4. These measurements are performed for laser light on resonance with the optical cavity and for input signal powers

reflected signal, showing the cavity-laser detuning (dashed line) locked to during squeezing measurements. **c**, Homodyne noise PSD of the reflected signal showing the transduced thermal Brownian motion of the zipper cavity at $T_{\rm b}=16$ K (green curve; $\langle n_c\rangle=80$). The red curve is the shot-noise level and the black curve is the detector's dark noise (in the absence of light input). Inset, close-up of the fundamental in-plane differential mechanical mode of the zipper cavity (fitted by blue curve; linewidth, $\gamma_i/2\pi=172$ Hz). **d**, Mean value of the PSD of the BHD as a function of the local-oscillator (LO) power (signal blocked). The filled data point indicates the local-oscillator power used in the squeezing measurements. The red and dashed black curves correspond to a linear fit to the data and the level of the detector dark current, respectively. **e**, Noise PSD as a function of $\theta_{\rm lock}$ (ranging from 0 (green) to π (red)) with the signal detuned far off resonance at $\Delta/\kappa\approx30$, referenced to the noise level with the signal blocked (blue).

varying from 252 nW to 3.99 μ W, with the maximum signal power corresponding to an average intracavity photon number of $\langle n_c \rangle = 3,153$. The laser is set at the appropriate cavity detuning for each signal power by scanning the wavelength across the cavity resonance while monitoring the reflection, and then stepping the laser frequency towards the cavity from the long-wavelength side until the reflection matches the level that corresponds to a detuning of $\Delta_{lock}/\kappa = 0.044 \pm 0.006$. This produces a shift of $\phi = (0.73 \pm 0.03)\pi$ in the measured quadrature angle from the on-resonance condition of equations (1)–(3) (Methods Summary).

In Fig. 3, we plot the theoretically predicted and measured noise PSDs versus quadrature angle for a signal power corresponding to $\langle n_c \rangle = 790$ photons. Each quadrature spectrum is the average of 150 traces, and after every other spectrum the signal arm is blocked and the shot-noise PSD is measured. The shot-noise level, corresponding to optical vacuum on the signal arm, is used to normalize the spectra. At certain quadrature angles, and for frequencies a few megahertz around the mechanical resonance frequency, we find that the light reflected from the zipper cavity shows a noise PSD below that of vacuum. The density plot of the theoretically predicted noise PSD (Fig. 3a) shows the expected wideband squeezing due to the strong optomechanical coupling in these devices, as well as a change in the phase angle where squeezing is observed below and above the mechanical frequency. This change is due to the change in sign of the mechanical susceptibility and the corresponding change in phase of the mechanical response to

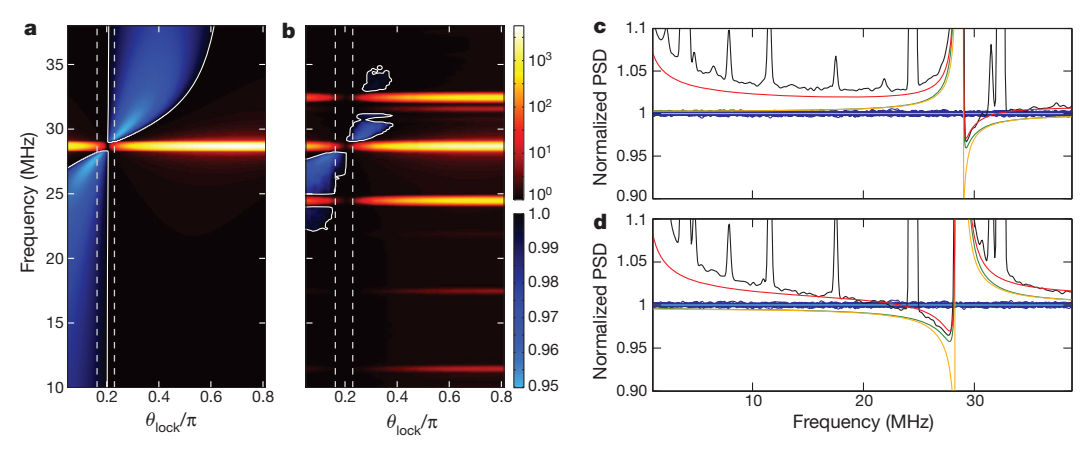


Figure 3 | Optomechanical squeezing of light. a, Theoretical model. Density plot of the predicted reflected-signal noise PSD, as measured on a balanced homodyne detector and normalized to shot-noise, for a simplified model of the optomechanical system (Supplementary Information). Areas with noise below shot-noise are shown in blue shades on a linear scale. Areas with noise above shot-noise are shown in orange shades on a log scale. The solid white line is a contour delineating noise above and below shot-noise. b, Experimental data. Density plot of the measured reflected-signal noise PSD for $\langle n_c \rangle = 790$, normalized to the measured shot-noise level. c, Slice of the measured density

plot in **b** taken at $\theta_{lock}/\pi=0.23$. **d**, Slice of the measured density plot in **b** taken at $\theta_{lock}/\pi=0.16$. In **c** and **d**, the black curve corresponds to the measured data slice extracted from **b**. The dark blue traces are several measurements of the shot-noise level (average shown in light blue). Also shown is a model of the squeezing in the absence of thermal noise (orange curve), the same model with ohmic thermal noise of the mechanical mode included (green) and a full noise model including additional phenomenological noise sources (red curve). The vertical white dashed lines in **a** and **b** indicate the data slices shown in **c** and **d**.

RPSN. The measured noise PSD density plot (Fig. 3b) shows the presence of several other mechanical noise peaks and a reduced squeezing bandwidth, yet the overall phase- and frequency-dependent characteristics of the squeezing around the strongly coupled in-plane mechanical mode are clearly present. In particular, Fig. 3c and Fig. 3d show two slices of the noise PSD density plot in which the region of squeezing changes from being below the mechanical resonance frequency to being above it.

In Fig. 4a, we show the measured noise PSD as a function of quadrature angle for a frequency slice at $\omega/2\pi=27.9\,\mathrm{MHz}$ of the data shown in Fig. 3b. The measured squeezing and anti-squeezing are seen to be smaller and, respectively, larger than expected from a model of the optomechanical cavity without thermal noise. We also plot, in Fig. 4b, the maximum measured and modelled squeezing as functions of signal power. The simple theory predicts a squeezing level that monotonically increases with signal power, whereas the measured maximum squeezing saturates at a level of $4.5\pm0.2\%$ below the shot-noise at an intracavity power corresponding to $\langle n_c \rangle = 1,984$ photons. The error in the squeezing is dominated by the uncertainty in the linearity of the detector gain ($\pm0.15\%$) and the variance of the measured shot-noise level ($\pm0.1\%$).

To understand the processes that limit the bandwidth and magnitude of the measured squeezing, we plot in Fig. 4c the noise PSD for phase quadratures that maximize (left plot) and minimize (right plot) the transduction of the mechanical mode peak. Along with the measured data, we also plot the estimated noise due to phase noise of the signal laser, and that for a model of a single mechanical mode coupled to a thermal bath at $T_{\rm b}=16\,{\rm K}$. Low-frequency noise in the motion quadrature shows an ω^{-1} frequency dependence consistent with structural damping effects30, but is much larger than that of the single-mode noise model. Noise in the quadrature that minimizes transduced motion is orders of magnitude larger than the noise predicted by the single-mode model and laser phase noise, and shows an $\omega^{-1/2}$ frequency dependence. The optical power dependence of the low-frequency noise in the motion quadrature indicates that optical absorption heats the structure to $T_{\rm b} \approx 30\,{\rm K}$ at the highest measured powers. As detailed in Supplementary Information, the red curve in each of the plots in Fig. 4 shows a full noise model incorporating structural damping noise from higher-frequency mechanical modes, optical absorption heating and a phenomenological $\omega^{-1/2}$ noise term.

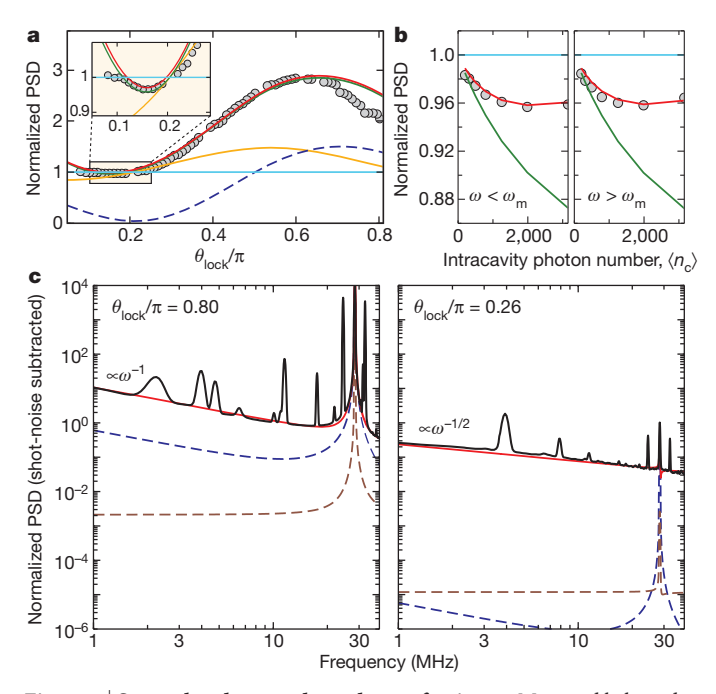


Figure 4 | Spectral and power dependence of noise. a, Measured balanced homodyne noise power of the reflected signal at $\omega/2\pi=27.9\,\text{MHz}$ (filled circles) versus quadrature angle ($\Delta_{lock}/\kappa = 0.044$ and $\langle n_c \rangle = 790$). The green and red curves correspond to the single-mode and full noise models, respectively. The orange curve represents a model including the response of the mechanical mode in the absence of thermal noise, that is, when driven by RPSN only, and the dashed blue curve shows the thermal noise component. Inset, close-up of boxed region. b, Measured minimum noise PSD normalized to shot-noise (filled circles) versus $\langle n_c \rangle$. Left: maximum squeezing for $\omega < \omega_m$; right: maximum squeezing for $\omega > \omega_m$. Also shown are the single-mode noise model (green curve) and the full noise model (red curve). c, Balanced homodyne noise PSD of the reflected cavity signal for Δ_{lock} $\kappa = 0.052$ and $\langle n_c \rangle = 3{,}153$. Left: phase quadrature corresponding to maximum transduction of mechanical motion; right: phase quadrature corresponding to minimum transduction of mechanical motion. In each plot, the black curve is the measured data with the shot-noise level subtracted. Also shown are the modelled laser phase noise (dashed brown curve), the noise contribution from a single mechanical mode (dashed blue curve) and the full noise model (red curve).

These models indicate that the currently obtainable levels of squeezing are limited by the thermal noise of higher-order mechanical modes.

These measurements show that by reflecting light off a thin-film mechanical resonator undergoing large-amplitude thermal motion, light that is in certain respects 'quieter' than vacuum can be obtained. In contrast to previous work with ultracold gas-phase atoms⁶, which used a narrowband atomic resonance and operated in short bursts owing to the atomic trap lifetime, the solid-state devices in this work allow for steady-state squeezing over almost 10 MHz of bandwidth and at optical frequencies completely tailorable through geometric design. The modest level of squeezing, limited by thermal noise and structural damping effects in the current devices, may also be substantially improved by increasing the mechanical Q-factor. Measurements of similar silicon devices with different surface treatments have yielded mechanical Q-factors as high as 7×10^5 (Supplementary Information), which, for the optical power levels used here, should enable on-chip squeezing 6 dB below shot-noise. Given the integrability of these microchip devices, optical extraction inefficiencies can be avoided by sending the squeezed light generated by one device directly into a second probe device. For example, such an on-chip squeezer and detector could form the basis of a quantum-enhanced micromechanical displacement and force sensor¹⁷. More generally, we expect these sorts of device to enable future experiments involving feedback and strong measurement of the dynamics of a mechanical system.

METHODS SUMMARY

Experimental set-up. A tunable external-cavity diode laser, actively locked to a wavemeter, is used to generate a strong local oscillator and the measurement signal. Fractions of the local oscillator and input signals are split off and detected, using intensity modulators to stabilize their power levels. Fibre polarization controllers adjust the polarization of the local oscillator and signal. A variable optical attenuator is used to set the signal power and an acousto-optic modulator is used to generate a tone for calibration (Supplementary Information). The reflected signal from the cavity is separated using a circulator, and is switched between one of three detection paths: one contains a power meter for power calibration, one contains a photodetector (PD1) for spectroscopy of the cavity and one contains an erbium-doped fibre amplifier for measurement of the mechanical spectrum on a real-time spectrum analyser or a network analyser. Squeezing of the reflected cavity signal is measured on a fourth path containing a variable coupler, where the signal is recombined with the local oscillator and detected on a balanced homodyne detector.

Homodyne phase angle. The relative phase between the local oscillator and the signal is determined from the low-pass-filtered component of the signal detected using a balanced homodyne detector, and set using a fibre stretcher. Locking the level of this signal determines the phase angle between the local oscillator and the reflected signal, which we call $\theta_{\rm lock}$. This angle differs from the phase θ between the light input to the cavity and the local oscillator, but is related to it through the phase response of the cavity: $\theta_{\rm lock} = \theta - \phi$, where $\phi(\Delta) = {\rm Arg}[1 - \kappa_e/(i\Delta + \kappa/2)]$ and κ_e is the extrinsic cavity coupling rate.

Cavity lock. A lock point slightly red detuned from resonance is chosen to avoid instabilities of the system resulting from thermo-optical effects. The laser is locked to this frequency using a wavemeter with a frequency resolution of $\pm 0.0015\kappa$. Drift of the optical cavity resonance over a single noise spectrum measurement (order of minutes) is found to be negligible. An estimate of the variance of $\Delta_{\rm lock}$ is determined from the dependence of the transduction of the mechanical motion on the quadrature phase, which indicates that from one lock to another $\Delta_{\rm lock}/\kappa = 0.044 \pm 0.006$.

Received 25 February; accepted 16 May 2013.

- 1. Braginsky, V. & Khalili, F. Quantum Measurements (Cambridge Univ. Press, 1995).
- Clerk, A. A., Devoret, M. H., Girvin, S. M., Marquardt, F. & Schoelkopf, R. J. Introduction to quantum noise, measurement, and amplification. *Rev. Mod. Phys.* 82, 1155–1208 (2010).
- Caves, C. M. Quantum-mechanical noise in an interferometer. Phys. Rev. D 23, 1693–1708 (1981).

- Fabre, C. et al. Quantum-noise reduction using a cavity with a movable mirror. Phys. Rev. A 49, 1337–1343 (1994).
- Mancini, S. & Tombesi, P. Quantum noise reduction by radiation pressure. Phys. Rev. A 49, 4055–4065 (1994).
- Brooks, D. W. C. et al. Non-classical light generated by quantum-noise-driven cavity optomechanics. Nature 488, 476–480 (2012).
- Yuen, H. P. Two-photon coherent states of the radiation field. Phys. Rev. A 13, 2226–2243 (1976).
- Hollenhorst, J. N. Quantum limits on resonant-mass gravitational-radiation detectors. *Phys. Rev. D* 19, 1669–1679 (1979).
- 9. Walls, D. F. Squeezed states of light. Nature 306, 141-146 (1983).
- Slusher, R. E., Hollberg, L. W., Yurke, B., Mertz, J. C. & Valley, J. F. Observation of squeezed states generated by four-wave mixing in an optical cavity. *Phys. Rev. Lett.* 55, 2409–2412 (1985).
- Shelby, R. M., Levenson, M. D., Perlmutter, S. H., DeVoe, R. G. & Walls, D. F. Broadband parametric deamplification of quantum noise in an optical fiber. *Phys. Rev.* Lett. 57, 691–694 (1986).
- Wu, L.-A., Kimble, H. J., Hall, J. L. & Wu, H. Generation of squeezed states by parametric down conversion. *Phys. Rev. Lett.* 57, 2520–2523 (1986).
- Grangier, P., Slusher, R. E., Yurke, B. & LaPorta, A. Squeezed-light-enhanced polarization interferometer. *Phys. Rev. Lett.* 59, 2153–2156 (1987).
- Mehmet, M. et al. Squeezed light at 1550 nm with a quantum noise reduction of 12.3 dB. Opt. Express 19, 25763–25772 (2011).
- The LIGO Scientific Collaboration. A gravitational wave observatory operating beyond the quantum shot-noise limit. Nature Phys. 7, 962–965 (2011).
- Taylor, M. A. et al. Biological measurement beyond the quantum limit. Nature Photon. 7, 229–233 (2013).
- Hoff, U. B. et al. Quantum-enhanced micromechanical displacement sensitivity. Opt. Lett. 38, 1413–1415 (2013).
- Caves, C. M. Quantum-mechanical radiation-pressure fluctuations in an interferometer. *Phys. Rev. Lett.* 45, 75–79 (1980).
- 19. Abbott, B. et al. Observation of a kilogram-scale oscillator near its quantum ground state. N. J. Phys. 11, 073032 (2009).
- Teufel, J. D. et al. Sideband cooling of micromechanical motion to the quantum ground state. Nature 475, 359–363 (2011).
- Gigan, S. et al. Self-cooling of a micromirror by radiation pressure. Nature 444, 67–70 (2006).
- Arcizet, O., Cohadon, P.-F., Briant, T., Pinard, M. & Heidmann, A. Radiation-pressure cooling and optomechanical instability of a micromirror. *Nature* 444, 71–74 (2006)
- Corbitt, T., Ottaway, D., Innerhofer, E., Pelc, J. & Mavalvala, N. Measurement of radiation-pressure-induced optomechanical dynamics in a suspended Fabry-Perot cavity. *Phys. Rev. A* 74, 021802 (2006).
- Murch, K. W., Moore, K. L., Gupta, S. & Stamper-Kurn, D. M. Observation of quantum-measurement backaction with an ultracold atomic gas. *Nature Phys.* 4, 561–564 (2008).
- Eichenfield, M., Camacho, R., Chan, J., Vahala, K. J. & Painter, O. A picogram- and nanometre-scale photonic-crystal optomechanical cavity. *Nature* 459, 550–555 (2009).
- 26. Chan, J. et al. Laser cooling of a nanomechanical oscillator into its quantum ground state. *Nature* **478**, 89–92 (2011).
- Gardiner, C. W. & Collett, M. J. Input and output in damped quantum systems: quantum stochastic differential equations and the master equation. *Phys. Rev. A* 31, 3761–3774 (1985).
- Purdy, T. P., Peterson, Ř. W. & Regal, C. A. Observation of radiation pressure shot noise on a macroscopic object. Science 339, 801–804 (2013).
- Verhagen, E., Deléglise, S., Weis, S., Schliesser, A. & Kippenberg, T. J. Quantumcoherent coupling of a mechanical oscillator to an optical cavity mode. *Nature* 482, 63–67 (2012).
- Liu, Y. T. & Thorne, K. S. Thermoelastic noise and homogeneous thermal noise in finite sized gravitational-wave test masses. *Phys. Rev. D* 62, 122002 (2000).

Supplementary Information is available in the online version of the paper.

Acknowledgements We would like to thank K. Hammerer and A. A. Clerk for discussions. This work was supported by the DARPA/MTO ORCHID programme through a grant from the AFOSR; the Institute for Quantum Information and Matter, an NSF Physics Frontiers Center with support of the Gordon and Betty Moore Foundation; the Vienna Science and Technology Fund WWTF; the European Commission, through IP SIQS and iQUOEMS; and the European Research Council. A.H.S.-N. and J.C. gratefully acknowledge support from NSERC. S.G. acknowledges support from the European Commission through a Marie Curie Fellowship.

Author Contributions A.H.S.-N., S.G. and M.A. designed the experiment. A.H.S.-N., S.G., J.C. and J.T.H. designed and fabricated the device, and performed the measurements. A.H.S.-N., S.G., J.T.H. and O.P. performed the analysis and modelling of the data. All authors were involved in writing and editing the paper.

Author Information Reprints and permissions information is available at www.nature.com/reprints. The authors declare no competing financial interests. Readers are welcome to comment on the online version of the paper. Correspondence and requests for materials should be addressed to O.P. (opainter@caltech.edu).